

EVLA Memo #119

Wide-Band Sensitivity and Frequency Coverage of the EVLA and VLA L-Band Receivers

Rick Perley and Bob Hayward

January 17, 2008

Abstract

We determine the sensitivities of the EVLA and VLA antennas over their full tuning ranges through analysis of the correlation coefficients. Interim EVLA antennas can tune over the full range of 940 through 2200 MHz. The prototype L-band OMT shows good performance over its design frequency range. The better-performing interim EVLA antennas meet the Project Book sensitivity requirements above ~ 1150 MHz. VLA antennas are capable of tuning from 1225 through 1900 MHz, with some limited capability between 1100 and 1225 MHz.

1 Introduction

The EVLA Project Book specifies the required sensitivity for each of the EVLA bands. For L-band, these requirements are shown in Fig. 1. The ‘steps’ at each end are to allow for amplifier and feed ‘edge effects’.

In EVLA Memo#109, we reported on the wide-band performance of the EVLA’s L-band feed, utilizing total-power observations with hot and cold loads. The use of hot and cold loads, combined with observations of sources of known flux density permit a determination of the antenna gain (or efficiency) and system temperature. However, these measurements are time-consuming, and the need to use total power radiometry make the measurements very susceptible to external interference.

In many cases, the relevant quantity is not the antenna gain or system temperature, but rather their ratio, as this is the quantity which directly affects overall sensitivity. This ratio is much easier to measure than either of the factors, and indeed can easily be determined through analysis of correlation coefficients provided by the correlator for each antenna pair. The AIPS calibration algorithms can be employed to solve for the antenna sensitivities. This approach provides many advantages – ease of setup and measurement, the ability to simultaneously obtain all antenna sensitivities, and in many cases a considerable rejection of external interference.

This memo describes the method for determining the system sensitivity through use of the correlation coefficients, and utilizes this method to measure both the EVLA and VLA’s L-band sensitivity over their entire tuning ranges.

There are at this time three types of L-band antennas in the field – The old-style VLA antennas, ‘interim’ EVLA antennas, and a single prototype EVLA antenna. The differences between these are given in Table 1

	VLA	Interim EVLA	Prototype EVLA
OMT Design BW (MHz)	1200 – 1800	1200 – 1800	1000 – 2000
Phase-Shifter Type	Dielectric	90 deg. hybrid coupler	90 deg hybrid coupler
Phase-Shifter Location	In front of OMT (warm)	After OMT (cold)	After OMT (cold)
LNA-Type	Single Ended	Double-Balanced	Double-Balanced
LNA-BW (MHz)	1200 – 1800	1000 – 2000	1000 – 2000
Warm RF Filter BW (MHz)	NA	NA	1000 – 2000
Post-Amp BW (MHz)	1200 – 1800	1200 – 1800	1000 - 2000

Table 1: Showing the differences between VLA, Interim EVLA, and the Prototype EVLA antenna #14.

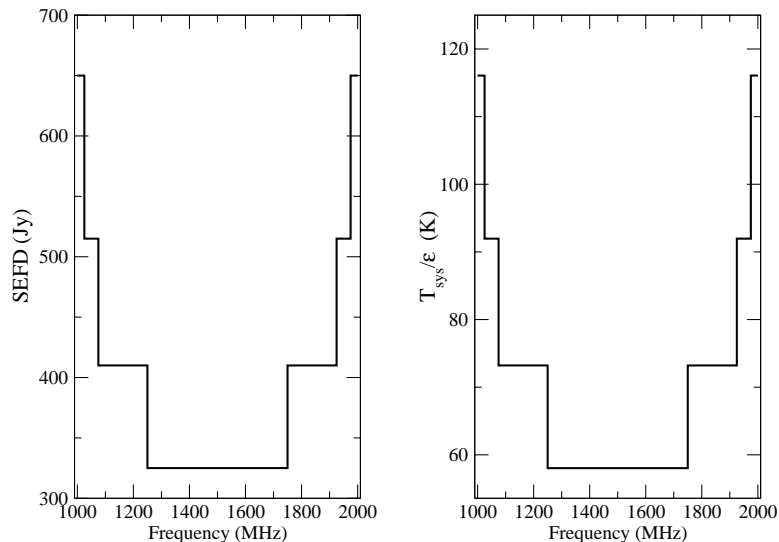


Figure 1: The project requirements on antenna sensitivity at L-band. The left panel expresses these in terms of the System Equivalent Flux Density (SEFD), the right panel in terms of the modified system temperature, T_{sys}/ϵ .

2 Method

For noise from a single antenna, the correlation coefficient is the ratio of the noise power due to the astronomical source to the total noise power:

$$\rho = \frac{P_A}{P_A + P_S} \quad (1)$$

where P_A is the source noise power, and P_S is the noise power not originating from the source. For an interferometer comprising two different elements, and expressing the powers in terms of the noise equivalent temperatures, this can be written as

$$\rho_{ij} = \frac{\sqrt{T_{A_i} T_{A_j}}}{\sqrt{(T_{A_i} + T_{S_i})(T_{A_j} + T_{S_j})}} \quad (2)$$

where the subscripts (i,j) denote the two component antennas.

In almost all cases, the antenna temperature due to the source is very much less than the uncorrelated noise temperature due to the electronic, atmosphere, and ground spillover. Making this approximation, assuming an unpolarized source, and expressing the antenna temperature in terms of the source flux density S and antenna collecting area A_p , through $T_A = S\epsilon A_p/2k$, we find

$$\rho_{ij} = \frac{SA_p}{2k} \sqrt{\frac{\epsilon_i}{T_{S_i}} \frac{\epsilon_j}{T_{S_j}}} \quad (3)$$

where ϵ is the antenna efficiency.

Bryan Butler, in AIPS Memo 108, has described how the VLA's correlator provides a scaled value of the correlation coefficient, r_{ij} , which is related to the true correlation coefficient via

$$\rho_{ij} = \frac{r_{ij}}{256\eta_c} = 4.83 \times 10^{-3} r_{ij}, \quad (4)$$

where the factor of 256 arises from an internal scaling, and $\eta_c = 0.809$ is the quantization efficiency of the VLA's 3-level correlator. (The correction for quantization is non-linear in general, but can be linearized in the limit of low correlation coefficient).

Equating the previous two expressions, and multiplying out the constants provides the following relationship relating the observed (scaled) raw correlation coefficient, r_{ij} , to the antenna efficiencies and system temperatures:

$$\sqrt{\frac{\epsilon_i}{T_{S_i}} \frac{\epsilon_j}{T_{S_j}}} = \frac{r_{ij}}{36.8 S_{Jy}} \quad (5)$$

where S_{Jy} is the spectral flux density of the observed source, expressed in units of Janskys.

The AIPS calibration machinery provides, via a least-squares analysis, the antenna-based amplitude coefficients needed to convert the correlation coefficient into the (known) source flux density. If we denote this coefficient by G^1 , the antenna sensitivity can then be expressed in terms of the amplitude gain coefficient as

$$\frac{T_{sys}}{\epsilon} = 36.8 G^2 \quad \text{K} \quad (6)$$

The System Equivalent Flux Density, $SEFD$, is a convenient measure of antenna sensitivity, and is related to the system temperature and effective antenna aperture via

$$SEFD = \frac{2kT_{sys}}{\epsilon A_p} \quad (7)$$

where ϵ is the antenna aperture efficiency, and A_p is the antenna physical aperture. From this, and converting to units of Jy, we find

$$SEFD = 206 G^2 \quad \text{Jy} \quad (8)$$

The SEFD is particularly useful for estimating array sensitivity, as the rms noise in an observation taken with N antennas, in a single polarization with bandwidth B Hz over time T seconds is

$$\sigma = \frac{SEFD}{\eta N \sqrt{BT}} \quad \text{Jy} \quad (9)$$

where $SEFD$ is an appropriate average over all N antennas, and η is the system efficiency (= 0.79 for the VLA, 0.91 for the EVLA)².

3 Measurements

We observed the calibrator source 3C48 in the early morning, and at mid-day, on January 8, 2008, covering the range of 945 to 2295 MHz in 10 MHz steps, in a program designed to fully map out the sensitivity functions for both EVLA and VLA antennas. The early morning observations were taken at an elevation of 65 degrees, those later the same day were at an elevation of 45 degrees. The purpose of the early morning observation was to minimize aircraft navigation interference. The VLA's response below 1210 MHz and above 1750 MHz is highly frequency dependent due to the influence of its polarizer – to better map these regions, a special observation was taken in November 2007, using a spectral line mode and 3.125 MHz bandwidth.

The correlator data were loaded into AIPS as raw correlation coefficients, and analyzed, following basic editing, in the manner described in the previous section.

4 Results

The results for the entire frequency band in RCP (IF ‘B’) are shown in Figure 2. This shows the effective system temperature T_{sys}/ϵ for three antennas: VLA antenna 15, typical of the best-performing VLA antennas, EVLA antenna 24, which is the most sensitive EVLA antenna, and EVLA antenna 14, which has been outfitted with the prototype orthomode transducer (OMT). The thick red stepped line shows the EVLA sensitivity requirements.

The EVLA antennas – except antenna 14, which has a 1.0 – 2.0 GHz RF filter not present in the ‘interim’ EVLA receivers, can tune with good sensitivity up to 2250 MHz. EVLA antenna 24 (solid blue line) meets the EVLA sensitivity requirements at all frequencies above 1150 MHz. The high system temperature of EVLA antenna 14, which is equipped with the prototype wideband OMT, is due primarily to resistive losses in the OMT. The production model is expected to be considerably better. A ‘close-up’ view of the low-frequency sensitivity for the EVLA antennas is shown in Fig. 3

The low frequency (less than 1200 MHz) performance of the VLA antennas bears closer inspection. These antennas include a narrowband dielectric phase shifter and a microwave lens, which effectively block radiation at most frequencies below 1200 MHz. A detailed plot of a few VLA antennas at the low end of the band is shown in Fig 4.

¹This is not the signal path power gain

²The VLA efficiency is 0.79, rather than 0.809, because of addition loss due to the waveguide blanking. The EVLA value is appropriate for WIDAR's 4-bit correlation mode.

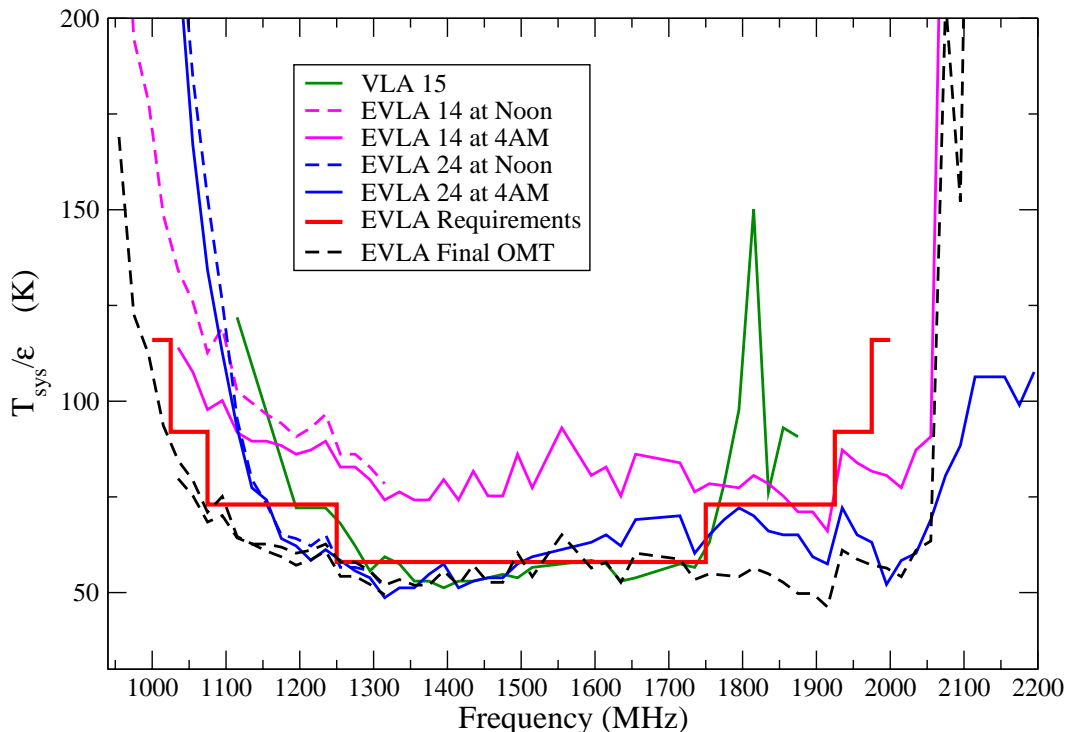


Figure 2: The VLA and EVLA antenna sensitivities, expressed in units of T_{sys}/ϵ over the entire L-band tuning range. The thick red line shows the EVLA’s Project Book requirements. VLA antenna 15 and EVLA antenna 24 are representative of the most sensitive antennas. EVLA antenna 14 is equipped with a prototype L-band OMT – the poorer sensitivity is believed due to resistive losses within the OMT. The dashed black line shows the expected sensitivity for the final system, including the optimized OMT.

In the ‘interim’ EVLA L-band receivers (such as antenna 24), the lens has been removed, and the dielectric phase-shifter has been replaced with a quadrature hybrid, so the performance loss at low frequencies is now due to the old-style OMT’s basic response. This is shown in Figure 3 by the blue solid and dashed lines. In antenna 14 however, the prototype OMT is in place, which provides dramatic improvement in low-frequency sensitivity, as shown by the solid magenta line. If the OMT resistive losses can be eliminated such that the high frequency performance is as good as antenna 24, we predict the low-frequency performance will be that shown by the dashed black lines – and will meet the project book requirements.

At the high-frequency end of the band, the EVLA antennas meet the sensitivity requirements with ease – even the especially noisy antenna 14. VLA antennas cannot tune above 1900 MHz due to LO limitations. All VLA antennas show a curious ‘spike’ in system temperature (or loss in efficiency) near 1800 MHz – the origin of which remains unknown, although we believe it is not due to the dielectric phase-shifter. These effects are shown in Figure 5.

5 Discussion

The results of this method can be directly compared to those obtained from the single-antenna tests. Figure 6 shows the SEFD values obtained by us from EVLA Memo 109 alongside our current results, on the same scales.

The agreement between these two methods is very impressive, and directly demonstrates the correctness of the correlation coefficient method. The very considerable advantage of the latter method is that it provides an easy-to-determine measurement for all antennas in the array simultaneously. However, this method cannot discriminate between a high system temperature and a low efficiency. To discriminate between these, direct antenna measurements with hot and cold loads will be required.

The sensitivity of the interim EVLA antennas over the very wide tuning range is very impressive. Although most do not yet meet the requirements at the low frequency end, continued development of the new wide-band OMT should ensure the required sensitivity in this frequency range.

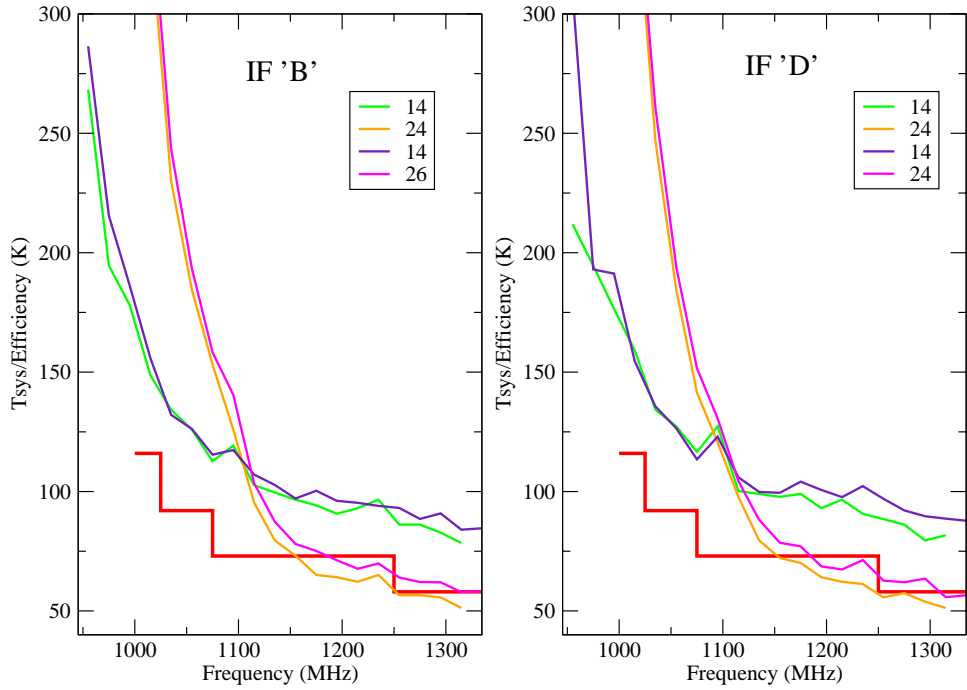


Figure 3: EVLA antennas 14 and 24 sensitivities between 950 and 1300 MHz, taken on two different afternoons. Antenna 14 contains the prototype OMT, while antenna 14 is the best performing interim EVLA antenna. Most of the difference in system temperature is due to losses within the OMT, which are expected to be largely eliminated in the production model. The faster rise of system temperature in antenna 24 below 1200 MHz is due to the VLA OMT. Observations were taken at 955, 975, ... MHz with 3 MHz BW – at no frequencies were any effects from the aircraft DME emissions detected in the visibilities.

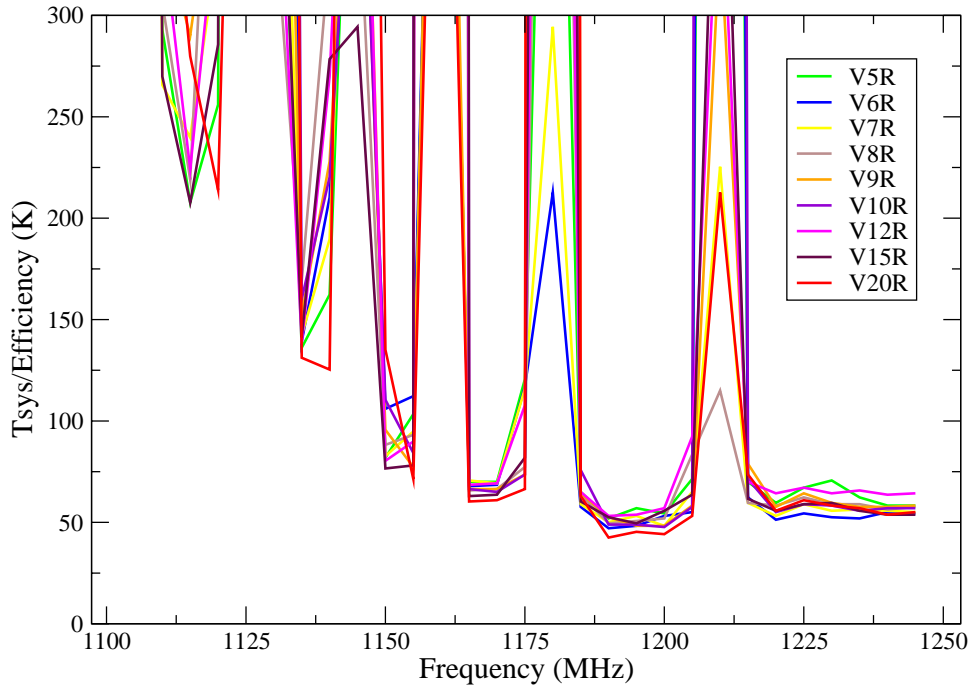


Figure 4: The VLA antenna sensitivities between 1100 and 1250 MHz. The ‘windows’ of poor sensitivity are caused by resonances within the VLA’s dielectric phase shifter and/or microwave lens.

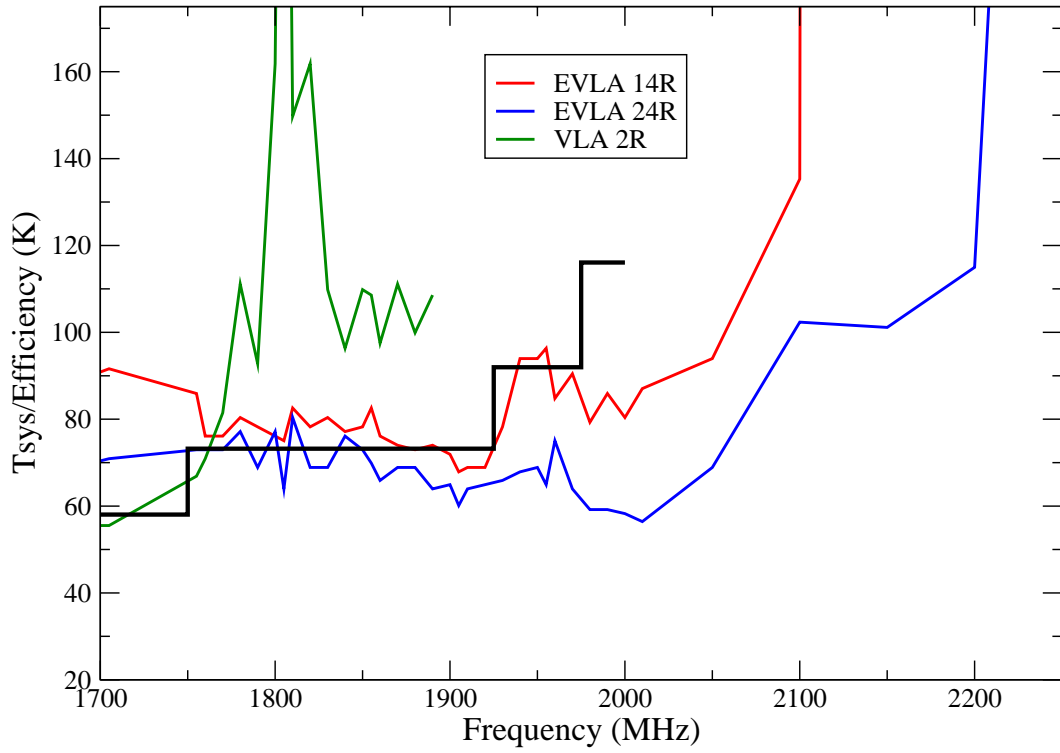


Figure 5: The VLA and EVLA antenna sensitivities, between 1700 and 2250 MHz. The notable rise between 1800 and 1825 MHz is a general feature for all VLA antennas, of unknown origin. The VLA can be effectively utilized up to 1900 MHz, albeit with reduced sensitivity. The EVLA performance remains very good all the way to 2200 MHz. The rise in T_{sys}/ϵ in the EVLA prototype antenna 14 is due to the 1–2 GHz filter in the warm IF subsystem.

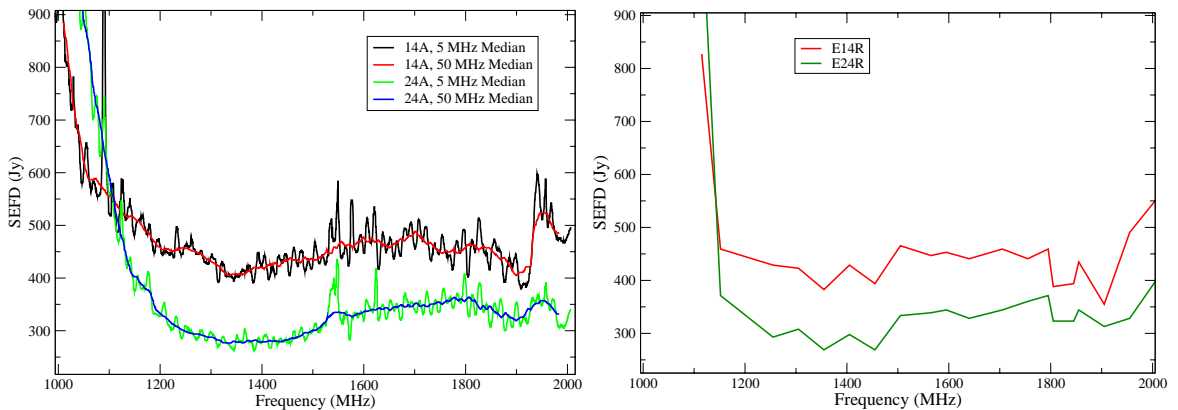


Figure 6: Comparing the SEFD values determined from single-antenna measurements (left) to those obtained from the current analysis, utilizing correlation coefficients, for IF ‘A’. Except for the abrupt rise at 1195 MHz (due to a power levelling problem), the agreement between the methods is excellent.

The good results shown here for frequencies outside of the standard L-band range – above 2.0 and below 1.0 GHz, generates a question on the optimal width of RF bandpass filters. The current plan is to insert in the RF path, following the first stage of amplification, bandpass filters whose purpose is to prevent out-of-band RFI from entering the IF electronics, and to maintain the required headroom by limiting the total power seen by the IF electronics. The specified filter widths for L and S bands are shown in the Table 2.

Att.	L-Band		S-Band	
	MHz	MHz	MHz	MHz
1dB	1000	2000	2000	4000
3dB	950	2080	1980	4100
30dB	780	2220	1560	4440
50dB	0650	3250	1100	4900

Table 2: The proposed RF filter widths in GHz for L and S bands.

The effect of the fixed filters will be to permanently disable access to frequencies outside the span. Are these filters really necessary, and if so, how wide should they be? Protecting the correlator from out-of-band signals is not an issue, as there are very sharp anti-aliasing filters located at the end of the IF signal path, immediately before the samplers. A good illustration of the choices involved is provided by consideration of the low-frequency end of L-band. There are strong scientific reasons to permit access as far below 1.0 GHz as the feed and OMT will permit scientifically useful sensitivities. This is likely to be at or perhaps even below 950 MHz. But with the current filter plan, a significant degradation of sensitivity will occur near this frequency, with access below it essentially ruled out. On the other hand, there are known very strong RFI emissions below 900 MHz which must be prevented from reaching the IF. The one of most immediate concern is the Verizon cell phone frequency near 880 MHz. Although it is likely the receivers will be protected from this by the OMT’s waveguide cutoff, it seems prudent to retain an RF filter, whose lower edge would be located between 900 and 950 MHz.

Finally, a comment on data quality within the aircraft aeronautical bands. Observations at L-band between 1025 and 1150 MHz are reputedly difficult or impossible, as this is the spectral region occupied by aircraft navigation transmission, notably DME signals. For a good understanding of these, see Rick Fisher’s fine memo (GB Electronics Division Internal Report #313). Spectral monitoring of the 1.0 – 2.0 GHz window has shown a notable decrease in these transmissions between local midnight as 6AM (as is to be expected), so our primary observations were taken near 4 AM, and clearly indicate that this portion of the spectrum may yet be useable for radio astronomy at these hours. But, followup observations of this spectral region were taken in mid-day, and (much to our considerable surprise) provided the same stable fringes, and nearly identical sensitivities, despite the increase in aircraft transmissions. This offers some hope that useful observations in this spectral region may be possible without having to employ heroic post-processing efforts. Further observations, following implementation of a few of the production OMTs, are warranted.